Progress In Electromagnetics Research, PIER 102, 15–30, 2010

PHOTONIC TRANSMISSION SPECTRA IN ONE-DIMENSIONAL FIBONACCI MULTILAYER STRUCTURES CONTAINING SINGLE-NEGATIVE METAMATERIALS

H. Rahimi

Physics Faculty
University of Tabriz
Tabriz, Iran

A. Namdar

Physics Department
Azarbaijan University of Tarbiat Moallem
Tabriz, Iran

S. Roshan Entezar and H. Tajalli

Physics Faculty
University of Tabriz
Tabriz, Iran

Abstract—We investigate the transmission properties of the Fibonacci quasiperiodic layered structures consisting of a pair of double positive (DPS), epsilon-negative (ENG) or/and mu-negative (MNG) materials. It is found that there exist the polarization-dependent transmission gaps which are invariant with a change of scaling and insensitive to incident angles. Analytical methods based on transfer matrices and effective medium theory have been used to explain the properties of transmission gaps of DPS-MNG, DPS-ENG and ENG-MNG Fibonacci multilayer structures.

1. INTRODUCTION

Recently, the metamaterials that exhibit simultaneously negative permittivity ϵ and permeability μ in a frequency band have attracted intensive studies due to their unique electromagnetic (EM) properties.

Corresponding author: H. Rahimi (h_rahimi@tabrizu.ac.ir).

They are also called the double-negative (DNG) materials or left-handed materials because the electric field, the magnetic field and the wave vector of an EM wave propagating in such a medium form a left-handed triplet [1–7]. In addition to the DNG materials, another metamaterial called the single-negative (SNG) material in which only one of the material parameters is negative deserve special attention. The SNG materials consist of the mu-negative (MNG) materials with $\mu < 0$ but $\epsilon > 0$, and the epsilon-negative (ENG) materials with $\epsilon < 0$ but $\mu > 0$ [8].

Most of previous works on the metamaterials focused on the certain unusual properties of wave propagation in a photonic crystal. It was shown that a one-dimensional photonic crystal (1DPC) composed of alternating slabs of ordinary double-positive (DPS) and DNG media can have a type of photonic bandgap (PBG) corresponding to zero averaged refractive index ($\bar{n}$) [9–12]. Moreover, it is well known that a 1DPC constituted by a periodic repetition of MNG and ENG layers can possess another type of photonic gap with effective phase (φ_{eff}) of zero [13–15]. When the periodicity of photonic crystal structure is broken, wave propagation is not described by Bloch states. The opposite extreme of a periodic system is a fully random structure. In the random systems waves undergo a multiple scattering process and are subject to unexpected interference effects [16]. Multiple wave scattering in disordered materials shows many similarities with the propagation of electrons in semiconductors [17]. One of the first phenomena studied in this context was coherent backscattering or weak localization of wave [18]. Knowledge on the propagation of waves in completely ordered and disordered structures is now rapidly improving, little is known about the behavior of waves in the huge intermediate regime between total order and disorder. This intermediate regime is valid in quasiperiodic structures.

Quasiperiodic structures are nonperiodic structures that are constructed by a simple deterministic generation rule. In a quasiperiodic system two or more incommensurate periods are superimposed, so that it is neither aperiodic nor a random system and therefore can be considered as intermediate the two [19, 20]. In other words, due to a long-range order a quasiperiodic system can form forbidden frequency regions called pseudo band gaps similar to the bandgaps of a photonic crystal and simultaneously possess localized states as in disordered media [21]. Among the various quasiperiodic structuress, the Fibonacci binary quasiperiodic structure has been the subject of extensive efforts in the last two decades. The Fibonacci multilayer structure is the well-known 1D quasiperiodic structure, its electronic properties has been well-studied since the discovery of the

quasi-crystalline phase in 1984 [22]. Wave through a structure in the Fibonacci sequence had also been studied in past decade, and recently the resonant states at the band edge of a photonic structure in the Fibonacci sequence are studied experimentally [23]. Studies of various aspects of wave propagation in the Fibonacci quasiperiodic structures carried out in Refs. [24–31] have considerably improved our understanding of wave transport in the Fibonacci quasiperiodic structures.

In this paper, we investigate the photonic transmission spectra in the Fibonacci quasiperiodic layered structures consisting of single negative metamaterials. We study three kinds of the Fibonacci quasiperiodic layered structures of DPS-MNG, DPS-ENG and ENG-MNG, with dispersive and lossless multilayer stacks. In these structures, with the help of transfer matrix method and effective medium theory, we show the transmission spectra of TE and TM waves for both normal and oblique incidences and for different layer scalings. It is shown that for both TE and TM polarizations with normal and oblique incidences, there exist the transmission gaps which are invariant with a change of scale and insensitive to the incident angles.

The rest of this paper is arranged as follows. In Section 2, we briefly introduce some theoretical details and transfer-matrix method for the calculation of the transmission spectra. The result and discussion are presented in Section 3. Finally, the paper ends with a conclusion.

2. MODEL AND NUMERICAL METHODS

Quasiperiodic photonic structures are defined by simple mathematical rules which generate non-periodic structures. The Fibonacci sequence is the chief example of long-range order without periodicity, and can be constructed from juxtaposing two building blocks A and B, according to the following deterministic generation rule: $S_{N+1} = \{S_{N-1}S_N\}$ for $N \geq 1$, with $S_0 = \{B\}$ and $S_1 = \{A\}$, and the generation rule is repeatedly applied to obtain: $S_2 = \{BA\}$, $S_3 = \{ABA\}$, $S_4 = \{BAABA\}$, etc. The number of layers is given by F_N, where F_N is the Fibonacci number obtained from recursive relation $F_N = F_{N-1}+F_{N-2}$, with $F_0 = F_1 = 1$. Geometrical arrangement of 1D the Fibonacci multilayer structure, which is embedded in air, is shown in Fig. 1. In this multilayer structure, the thicknesses of A and B are supposed to be d_A and d_B, respectively.

We intend to investigate the transmission properties of 1D Fibonacci multilayer structures constituted by the multilayers of DPS,

MNG and ENG materials. Generally, the metamaterials are dispersive, i.e., ϵ and μ are frequency dependent. These materials have different expressions of ϵ and μ accordingly. For MNG material, we suppose that ϵ and μ can be expressed as [9].

$$\epsilon = 1, \quad \text{and} \quad \mu(\omega) = 1 + \frac{3^2}{0.902^2 - \omega^2}, \tag{1}$$

where ω is frequency in GHz. Similarly, we can take ϵ and μ for ENG material as,

$$\epsilon = 1 + \frac{5^2}{0.9^2 - \omega^2} + \frac{10^2}{11.5^2 - \omega^2}, \quad \text{and} \quad \mu = 1, \tag{2}$$

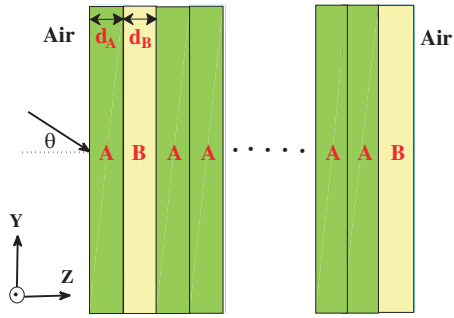

Figure 1. Schematic drawing of the one-dimensional quasiperiodic Fibonacci structure, which is embedded in air. The thicknesses of A and B are supposed to be d_A and d_B, respectively.

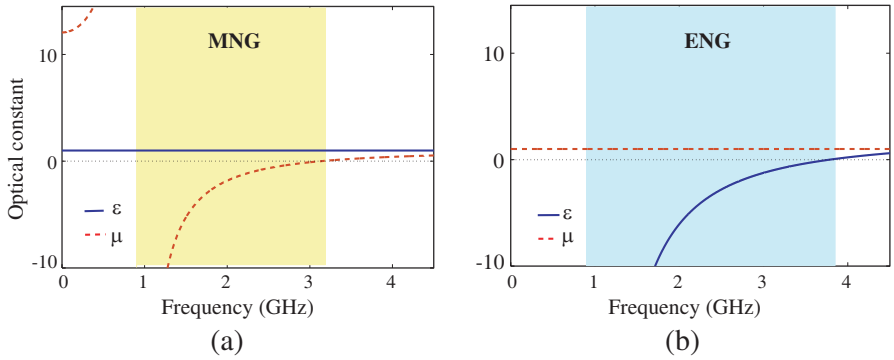

Figure 2. The permittivity ϵ (solid line) and the permeability μ (dashed line) of (a) MNG and (b) ENG materials as function of frequency.

For DPS material, both ϵ and μ are positive constants. Fig. 2 shows the optical constants (permittivities and permeabilities) of MNG and ENG materials. As one can see from Fig. 2, in the frequencies range 0.9–3.2 GHz, μ is negative and in the frequencies range 0.9–3.9 GHz, ϵ is negative. Also, for the frequencies greater than 3.9 GHz, both ϵ and μ are positive. In this work, since MNG and ENG metamaterials are considered in microwave frequency region, these layers are often electrically thin, i.e.,

$$\begin{aligned} |k_A|d_A &= \left| d_A \sqrt{\frac{\omega^2}{c^2}\left(\epsilon_A\mu_A - \sin^2\theta\right)} \right| \ll 1 \\ |k_B|d_B &= \left| d_B \sqrt{\frac{\omega^2}{c^2}\left(\epsilon_B\mu_B - \sin^2\theta\right)} \right| \ll 1, \end{aligned} \tag{3}$$

where c is the velocity of light in the vacuum. Also, ϵ_A and μ_A, likewise ϵ_B and μ_B are permittivity and permeability of two building blocks A and B, respectively. As a consequence, in the long-wavelength limit, we adopt effective medium approximation by introducing effective permittivity ϵ_{eff} and permeability μ_{eff} to study wave propagation in this Fibonacci multilayer structure. ϵ_{eff} and μ_{eff} of this nonperiodic structure are given by [32]

$$\begin{aligned} \mu_{eff} =& \frac{N_A d_A}{d}\mu_A + \frac{N_B d_B}{d}\mu_B, \\ \epsilon_{eff} =& \frac{N_A d_A}{d}\epsilon_A + \frac{N_B d_B}{d}\epsilon_B - \sin^2\theta\left(\frac{N_A d_A}{d}\frac{1}{\mu_A} + \frac{N_B d_B}{d}\frac{1}{\mu_B}\right) \\ &+ \sin^2\theta\left(\frac{1}{\frac{N_A d_A}{d}\mu_A + \frac{N_B d_B}{d}\mu_B}\right), \end{aligned} \tag{4}$$

for TE polarization and

$$\begin{aligned} \epsilon_{eff} =& \frac{N_A d_A}{d}\epsilon_A + \frac{N_B d_B}{d}\epsilon_B, \\ \mu_{eff} =& \frac{N_A d_A}{d}\mu_A + \frac{N_B d_B}{d}\mu_B - \sin^2\theta\left(\frac{N_A d_A}{d}\frac{1}{\epsilon_A} + \frac{N_B d_B}{d}\frac{1}{\epsilon_B}\right) \\ &+ \sin^2\theta\left(\frac{1}{\frac{N_A d_A}{d}\epsilon_A + \frac{N_B d_B}{d}\epsilon_B}\right), \end{aligned} \tag{5}$$

for TM polarization. In Eqs. (4) and (5), $d = N_A d_A + N_B d_B$ where N_A and N_B are the number of A-type and B-type slabs, respectively.

Eqs. (4) and (5) indicate that multilayer structure is anisotropic in essence because ϵ_{eff} and μ_{eff} depend on the incident angle θ.

In this paper, we take a certain level of the Fibonacci multilayer structure as a 1D multilayer structure to calculate the transmission spectra of this deterministic disorder structure. The transmission spectra of a layered system can be calculate by using transfer-matrix method. For this purpose, we assume that a wave be incident from air with angle θ onto the Fibonacci multilayer structure, shown in Fig. 1. For the transverse electric (TE) wave, the electric field E is assumed in the x direction (the dielectric layers are in the xy plane), and the z direction is normal to the interface of each layer. When such an electromagnetic wave propagates through this multilayer structure, the incident, reflected and transmitted electric fields are connected via a transfer matrix $\mathbf{M}$ as

$$\mathbf{M} = \begin{pmatrix} m_{11} & m_{12} \\ m_{21} & m_{22} \end{pmatrix}, \tag{6}$$

where $m_{ij}\,(i,j=1,2)$ is the element of the transfer matrix. For more details about this transfer matrix see Ref. [13]. For the Fibonacci structure with certain generation number (N), M can be calculated by a sequential product of the transfer matrices for every successive interface:

$$M_N = T_{airA}\; T_A\; T_{AB}\; T_B\; T_{BA}\; T_A\; T_A\; T_{AB}\; T_B\; \ldots\; T_B\; T_{Bair}, \tag{7}$$

where T_{airA} and T_{Bair} represent the propagation of light through the interface $air \rightarrow A$ and $B \rightarrow air$, respectively. T_A and T_B represent the propagation of light within layers A and B, respectively. Also, T_{AB} and T_{BA} represent the propagation of light through the interface $A \rightarrow B$ and $B \rightarrow A$, respectively. Eq. (8) cab be arranged for any order of the Fibonacci sequence S_N $(N \gg 3)$ as

$$M_N = T_{airA}\; T_N\; T_{Bair}, \quad \text{for } N_{even}, \tag{8}$$

$$M_N = T_{airA}\; T_N\; T_{Aair}, \quad \text{for } N_{odd}, \tag{9}$$

with,

$$T_N = T_{N-1}\; T_{N-2}, \qquad \text{for } N_{even}, \tag{10}$$

$$T_N = T_{N-1}\; T_{BA}\; T_{N-2}, \quad \text{for } N_{odd}, \tag{11}$$

whose initial conditions are

$$T_1 = T_A, \quad \text{and} \quad T_2 = T_A\; T_{AB}\; T_B. \tag{12}$$

The transmittance coefficients are given by

$$t = \left| \frac{1}{m_{11}} \right|^2 \tag{13}$$

The treatment of TM waves is similar to that for a TE waves.

3. RESULTS AND DISCUSSION

Here, we investigate three different combinations, DPS-MNG, DPS-ENG and MNG-ENG of dispersive and lossless materials as the Fibonacci multilayer structures. We find some band gaps whose properties are studied in this section in detail.

Firstly, we consider DPS-MNG Fibonacci multilayer structure, i.e., all A-type and B-type layers are DPS and MNG materials, respectively. In the following calculation, we choose $\epsilon_A = \mu_A = 1$, $d_A = 8\,\text{mm}$, $d_B = 4\,\text{mm}$ and the Fibonacci generation number $N = 14$. The frequency dependence of the effective permittivity ϵ_{eff} (solid line) and the effective permeability μ_{eff} (dashed line) of considered DPS-MNG structure are plotted in the Fig. 3 for both TE waves corresponding to the incident angles 0°, 20° (Figs. 3(a) and (b)) and TM waves with the incident angles 0°, 45° (Fig. 3(c)). The influence of the incident angle on the effective parameters ϵ_{eff} and μ_{eff} in the

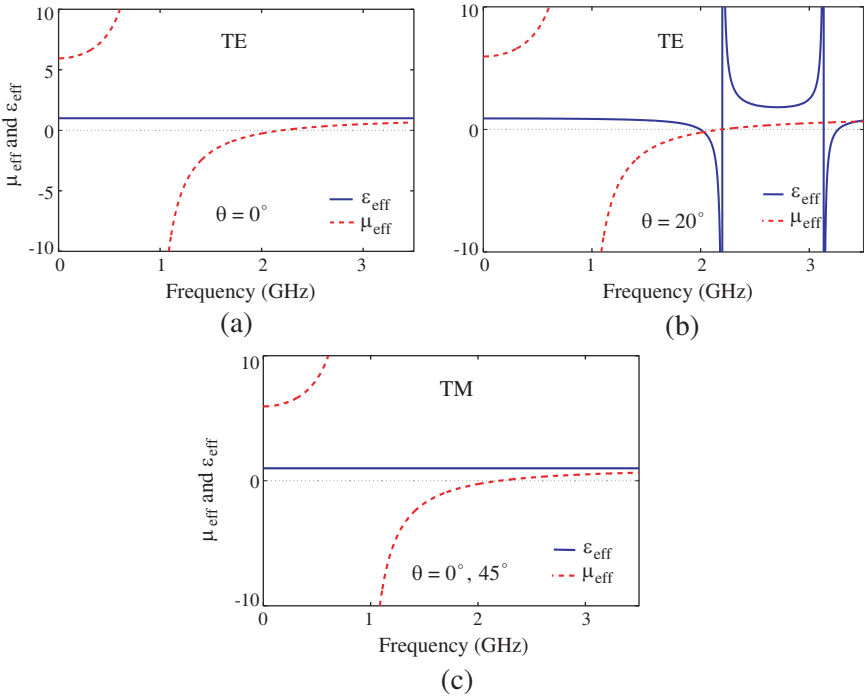

Figure 3. The effective permittivity ϵ_{eff} (solid line) and the effective permeability μ_{eff} (dashed line) of DPS-MNG Fibonacci structure for TE and TM waves, corresponding to the incident angles of 0°, 20° and 45° as indicated in plots.

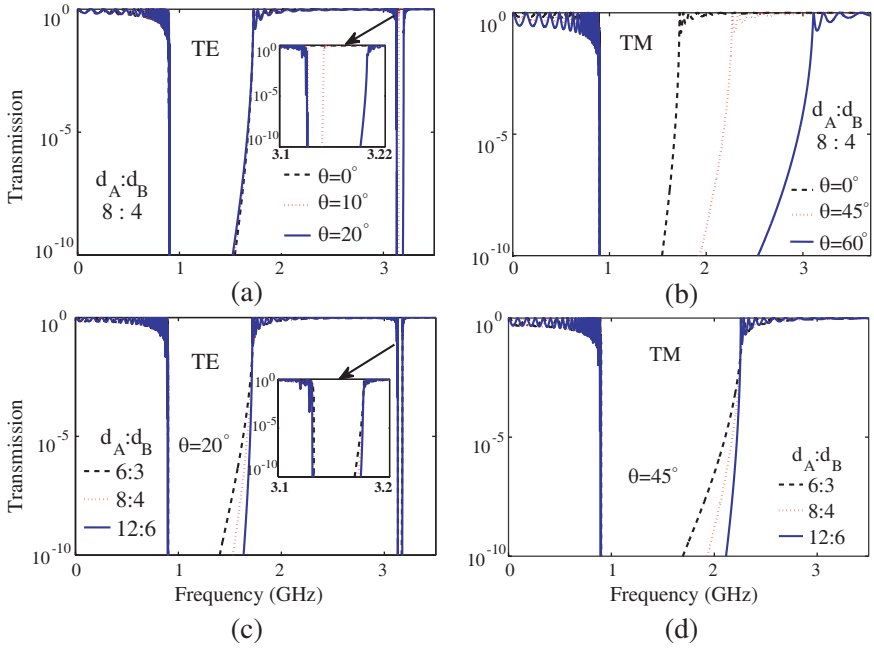

Figure 4. Transmission spectra of DPS-MNG Fibonacci structure for 14th Fibonacci level as a function of frequency for TE and TM waves with different incident angles; (a) $\theta = 0°$, $10°$ and $20°$, (b) $\theta = 0°$, $45°$ and $60°$ and with different thickness scales of $6:3$, $8:4$ and $12:6$ mm at (c) $\theta = 20°$, (d) $\theta = 45°$.

effective medium theory is introduced by expression $\sin^2\theta$ in Eqs. (4) and (5) for TE and TM modes, respectively. In our calculations for DPS-MNG Fibonacci structure when $\epsilon_A = \epsilon_B = 1$ the terms including $\sin^2\theta$ in Eq. (5) will cancel for TM modes, so ϵ_{eff} and μ_{eff} of DPS-MNG structure are independent of the incident angle for TM polarization (see Fig. 3(c)), whilst they are sensitive to the incident angle only for TE polarization (see Figs. 3 (a) and (b)).

The transmission spectra of TE and TM polarizations in DPS-MNG are represented for different incident angles of $\theta = 0°$, $20°$ and $45°$ and for different thickness scales as $d_A : d_B = 6:3$, $8:4$ and $12:6$ mm in Fig. 4. It is clear from Fig. 4(a) that there are two band gaps in the transmission spectra of TE waves. The first gap exists in the frequencies where the effective permeability μ_{eff} of structure is negative, whilst, the second gap is occurred in the frequencies where the effective permeability μ_{eff} of the structure is positive (see Fig. 3(a)). One can see from Fig. 4(a) that for TE polarization, the spectral width

of the first gap in this structure is invariant with a change in the incident angles, whilst, the spectral width of the second gap increases with the incident angle keeping left edge constant. The influence of the incident angle on the transmission property is introduced by wave vector $k = \frac{\omega}{c}\sqrt{\epsilon_{eff}\ \mu_{eff} - \sin^2\theta}$. Here, the dependence of transmission spectra on the incident angle is introduced by $\sin^2\theta$ and $\epsilon_{eff}(\theta)$ or/and $\mu_{eff}(\theta)$ for DPS-MNG Fibonacci structure. In the case of TM modes, since ϵ_{eff} and μ_{eff} are independent of the incident angle (see Fig. 3(c)), so the dependence of the transmission gap on the incident angle is reasonable as indicated in Fig. 4(b). In contrast with the TM modes, for TE modes the dependence of wave vector on the incident angle is introduced via $\epsilon_{eff}(\theta)$ and $\sin^2\theta$, so that the final result for k is independent (dependent) of incident angle in first (second) gap, hence transmission gap for TE mode will be independent (dependent) of incident angle in the first (second) gap as shown in Fig. 4(a).

Also, the second gap is found only for the oblique incidence and it disappears for the normal incidence. From Fig. 4(c), we can see that if the thicknesses of two building block $d_A = 8\,\text{mm}$ and $d_B = 4\,\text{mm}$ are scaled by 3/4 and 3/2, the position and width of the transmission gap are nearly invariant. It is seen from Figs. 4(b) and 4(d) that, for TM waves, only the first gap exists while the second gap corresponding to TE waves does not appear. The width of this first gap for TM waves increases with the angle of incidence but remains invariant with the scaling of d_A and d_A.

The second Fibonacci quasiperiodic layered structure (with generation number $N = 14$) consists of two stacking layers of DPS (with $\epsilon_A = \mu_A = 1$) and ENG materials having thicknesses $d_A = 8\,\text{mm}$, $d_B = 4\,\text{mm}$, respectively. the frequency dependence of the effective permittivity ϵ_{eff} (solid line) and the effective permeability μ_{eff} (dashed line) of considered DPS-ENG Fibonacci structure are demonstrated in the Fig. 5 for both TE waves with incident angles of 0°, 45° (Fig. 5(a)) and TM waves with incident angles of 0°, 20° (Figs. 5(b) and (c)). In DPS-ENG Fibonacci structure with $\mu_A = \mu_B = 1$ the terms including $\sin^2\theta$ in Eq. (4) will cancel for TE modes, so ϵ_{eff} and μ_{eff} are independent of the incident angle for TE polarization (Fig. 5(a)), whilst they are sensitive to the incident angle for TM polarization (Figs. 5(b) and (c)).

The Fig. 6 represents the transmission characteristics of DPS-ENG Fibonacci multilayer structure. In the case of TE polarization, as seen from Fig. 6(a), only one gap is found for considered structure in the frequency range corresponding to ENG material, so that, the upper edge of this gap is highly sensitive to the incident angle and increases when angle of incidence increases. Also, the middle of the spectral

width of this gap remains at the frequency rang that the corresponding effective permeability μ_{eff} of structure is negative (see Fig. 5) and the gap remains invariant when d_A and d_B are scaled by different values (see Fig. 6(c)). Additionally, one can see from Figs. 6(b) and 6(d) that, two band gaps are found for TM modes in the transmission spectra. The first (or second) gap appears in the frequency range where the effective permeability μ_{eff} is negative (positive) (see Fig. 5). The spectral width and position of the first gap do not change and remain invariant with a change of the incident angle and layer scale (see Figs. 6(b) and (d)). However, the second gap is sensitive to the incident angle and disappears for the normal incidence and it is invariant with a change of layer scale. The dependence of transmission spectra on the incident angle in DPS-ENG and ENG-MNG can be explained by similar discussion presented for DPS-MNG structure based on the effective medium theory.

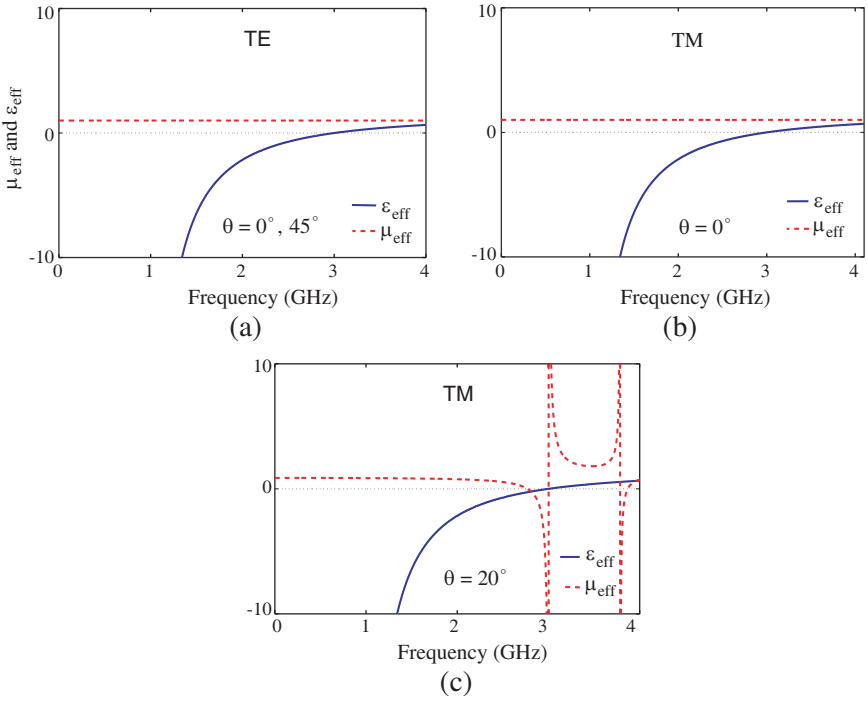

Figure 5. The effective permittivity ϵ_{eff} (solid line) and the effective permeability μ_{eff} (dashed line) of DPS-ENG Fibonacci structure for TE and TM waves, corresponding to the incident angles 0°, 20° and 45° as indicated in plots.

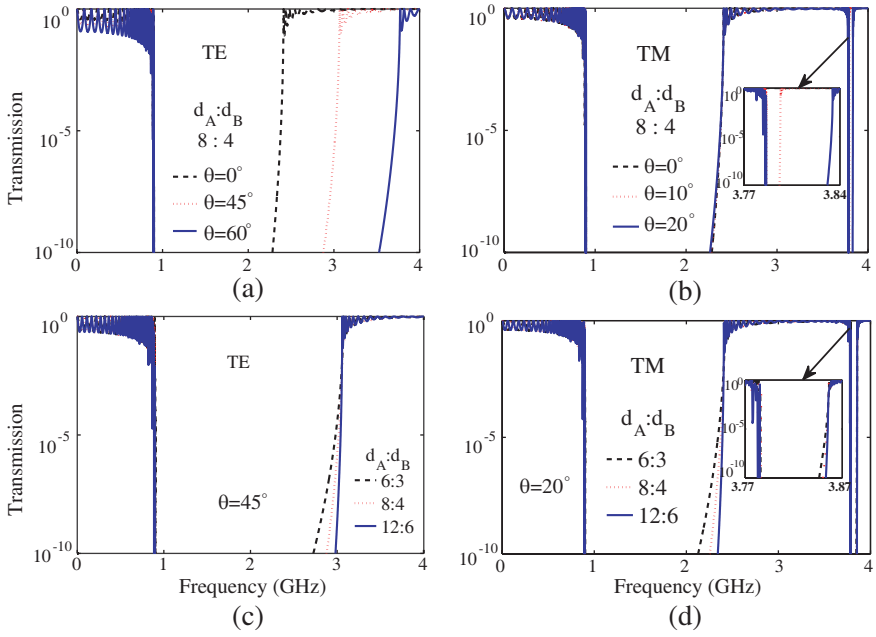

Figure 6. Transmission spectra of DPS-ENG Fibonacci structure for 14th Fibonacci level as a function of incident frequency corresponding to the incident angles 0°, 45° and 60° for TE waves and 0°, 10° and 20° for TM waves and for different thicknesses as $d_A : d_B = 6 : 3,\ 8 : 4$ and $12 : 6$ mm.

The third Fibonacci structure under investigation is composed of ENG (with $d_A = 8$ mm) and MNG (with $d_B = 4$ mm) materials. The effective permittivity ϵ_{eff} and the effective permeability μ_{eff} of this structure and the transmission spectra for the 14th Fibonacci level are shown in Figs. 7 and 8, respectively for TE and TM waves with different incident angles. It is seen from Fig. 7 that unlike DPS-MNG structure, in this case the μ_{eff} are sensitive to the incident angle for TM polarization. Also, in contrast with DPS-ENG structure, in this case the ϵ_{eff} are sensitive to the incident angle for TE polarization. It should be noted that the effective response of ENG-MNG structure in the normal incidence is identical for TE and TM waves. In the Fig. 8, the transmission spectra of TE and TM polarizations are plotted for the incidence angles $\theta = 0°,\ 30°$ and $45°$ and for three ratios of thicknesses $d_A : d_B = 6 : 3,\ 8 : 4$ and $12 : 6$ mm (at $\theta = 30°$). Regarding to the common frequency range corresponding to ENG and MNG materials of the structure, e.g., 0.9–3.2 GHz, we observe only

one gap in transmission spectra which is invariant with the angle of incidence and layer scaling for both TE and TM polarization. Indeed, the second gaps appeared in the transmission spectra which are highly sensitive to angles of incidence and insensitive to scaling are located out of the considered frequency range of ENG-MNG structure.

It is necessary to mention that in DPS-MNG, DPS-ENG and ENG-MNG structures, we studied the transmission spectra in 1D Fibonacci multilayer structures against generation number N. We found that there is a minimum generation number $N = 9$ in which the Fibonacci structure yield the photonic bandgap with sharp gap edges. But by decreasing generation number to the low values the photonic bandgap property of structure will disappear while, in the high number of N we have desirable gaps regardless to N is odd or even number.

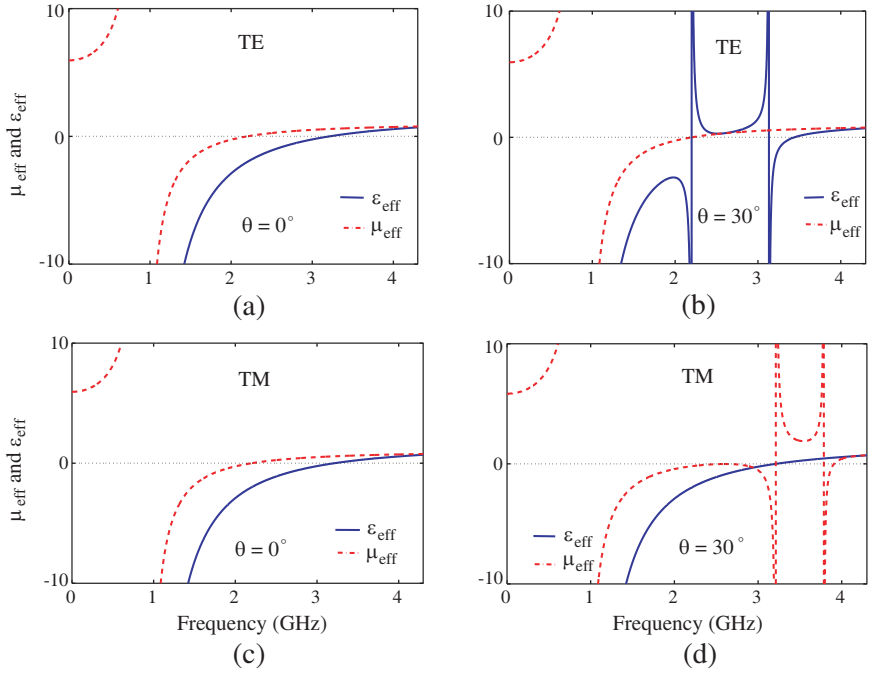

Figure 7. The effective permittivity ϵ_{eff} (solid line) and the effective permeability μ_{eff} (dashed line) of ENG-MNG Fibonacci structure for TE and TM waves, corresponding to the incident angles 0°, and 30°.

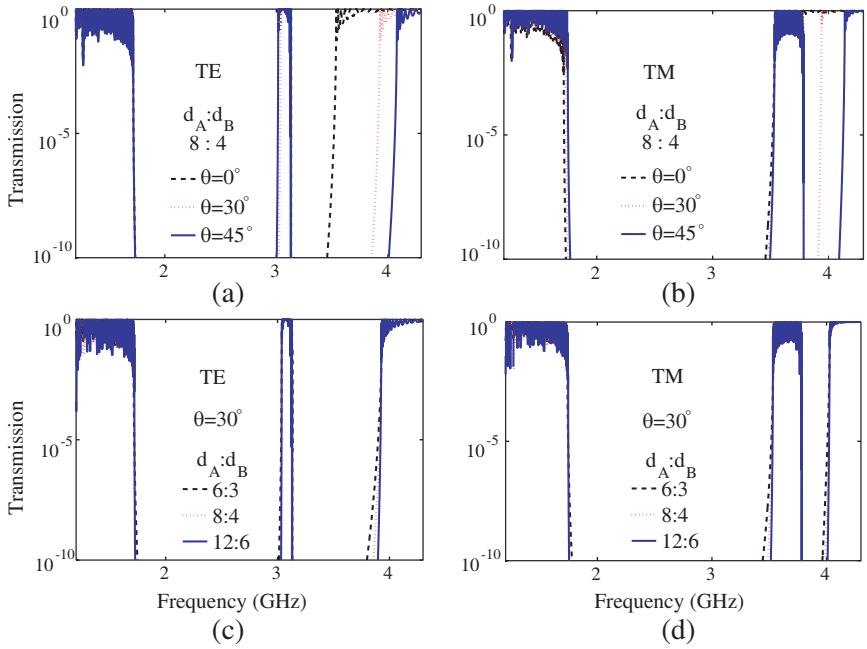

Figure 8. Transmission spectra of ENG-MNG Fibonacci structure for 14th Fibonacci level as a function of incident frequency for TE and TM waves corresponding to the incident angles 0°, 30° and 45°, and three thicknesses $d_A : d_B = 6 : 3,\ 8 : 4$ and $12 : 6$ mm.

4. CONCLUSION

In conclusion, based on the transfer-matrix method and effective medium theory, we have theoretically investigated the transmission spectra of three quasiperiodic Fibonacci layered structures consisting of dispersive and lossless MNG and ENG materials. In DPS-MNG, DPS-ENG, and ENG-MNG Fibonacci layered structures for both TE and TM waves, it is shown that there exist the transmission gaps which are invariant with a change of layer scale and insensitive to the incident angle. Moreover, for both TE and TM waves we have shown that, there is a gap which is only found at the oblique incidence, i.e., it disappears at the normal incidence.

REFERENCES

1. Veselago, V. G., "The electrodynamics of substance with stimultaneously negative values of ϵ and μ," *Sov. Phys. Usp.*, Vol. 10, 509, 1968.

2. Pendry, J. B., A. J. Holden, W. J. Stewart, and I. Youngs, "Extremely low frequency plasmons in metallic mesostructures," *Phys. Rev. Lett.*, Vol. 76, 4773–776, 1996.
3. Shelby, R. A., D. R. Smith, and S. Schultz, "Experimental verification of a negative index of refraction," *Science*, Vol. 292, 77, 2001.
4. Ran, L.-X., H.-F. Jiang Tao, H. Chen, X.-M. Zhang, K.-S. Cheng, T. M. Grzegorczyk, and J. A. Kong, "Experimental study on several left-handed metamaterials," *Progress In Electromagnetics Research*, PIER 51, 249–279, 2005.
5. Grzegorczyk, T. M. and J. A. Kong, "Review of left-handed metamaterials: Evolution from theoretical and numerical studies to potential applications," *Journal of Electromagnetic Waves and Applications*, Vol. 20, No. 14, 2053–2064, 2006.
6. Chen, H., B. I. Wu, and J. A. Kong, "Review of electromagnetic theory in left-handed materials," *Journal of Electromagnetic Waves and Applications*, Vol. 20, No. 15, 2137–2151, 2006.
7. Zainud-Deen, S. H., A. Z. Botros, and M. S. Ibrahim, "Scattering from bodies coated with metamaterial using FDFD method," *Progress In Electromagnetics Research B*, Vol. 2, 279–290, 2008.
8. Fredkin, D. R. and A. Ron, "Effectively left-handed (negative index) composite material," *Appl. Phys. Lett.*, Vol. 81, 1753, 2002.
9. Li, J., L. Zhou, C. T. Chan, and P. Sheng, "Photonic band gap from a stack of positive and negative index materials," *Phys. Rev. Lett.*, Vol. 90, 083901, 2003.
10. Srivastava, S. K. and S. P. Ojha, "Enhancement of omnidirectional reflaction bands in one-dimentional photonic crystals with left-handed materials," *Progress In Electromagnetics Research*, PIER 68, 91–111, 2007.
11. Srivastava, R., S. Pati, and S. P. Ojha, "Enhacement of omnidirectional reflection in photonic crystal hetrostructures," *Progress In Electromagnetics Research B*, Vol. 1, 197–208, 2008.
12. Srivastava, S. K. and S. P. Ojha, "Omnidirectional reflection bands in one-dimensional photonic crystal structure using fullerene films," *Progress In Electromagnetics Research*, PIER 74, 181–194, 2007.
13. Wang, L. G., H. Chen, and S. Y. Zhu, "Omnidirectional gap and defect mode of one-dimensional photonic crystals with single-negative materials," *Phys. Rev. B*, Vol. 70, 245102, 2004.
14. Jiang, H. T., H. Chen, H. Q. Li, Y. W. Zhang, J. Zi, and S. Y. Zhu, "Properties of one-dimensional photonic crystals

containing single-negative materials," *Phys. Rev. E*, Vol. 69, 066607, 2004.

15. Al, A. and N. Engheta, "Pairing an epsilon-negative slab with a mu-negative slab: Resonance, tunneling, and transparency," *IEEE Trans. Antennas Propag.*, Vol. 51, 2558, 2003.
16. Sheng, P., *Introduction to Wave Scattering, Localization and Mesoscopic Phenomena*, Academic Press, New York, 1995.
17. Merlin, R., K. Bajema, R. Clarke, F. Y. Juang, and P. K. Bhattacharya, "Quasiperiodic GaAs-AlAs heterostructures," *Phys. Rev. Lett.*, Vol. 55, 1768, 1985.
18. Albada, M. P. and A. Lagendijk, "Observation of weak localization of light in a random medium," *Phys. Rev. Lett.*, Vol. 55, 2692, 1985.
19. Jin, C. J., B. Y. Cheng, B. Y. Man, Z. L. Li, and D. Z. Zhang, "Two-dimensional dodecagonal and decagonal quasiperiodic photonic crystals in the microwave region," *Phys. Rev. B*, Vol. 61, 10762, 2000.
20. Kohmoto, M., B. Sutherland, and K. Iguchi, "Localization of optics: Quasiperiodic media," *Phys. Rev. Lett.*, Vol. 58, 2436, 1987.
21. Sheng, P., *Scattering and Localization of Classical Waves in Random Media*, World Scientific, Singapore, 1990.
22. Gellermann, W., M. Kohmoto, B. Sutherland, and P. C. Taylor, "Localization of light waves in Fibonacci dielectric multilayers," *Phys. Rev. Lett.*, Vol. 72, 633, 1994.
23. Dal Negro, L., C. J. Oton, Z. Gaburro, L. Pavesi, P. Johnson, A. Lagendijk, R. Righini, M. Colocci, and D. S. Wiersma, "Light transport through the band-edge states of Fibonacci quasicrystals," *Phys. Rev. Lett.*, Vol. 90, 055501, 2003.
24. Gumbs, G. and M. K. Ali, "Dynamical maps, cantor spectra, and localization for Fibonacci and related quasiperiodic lattices," *Phys. Rev. Lett.*, Vol. 60, 1081, 1988.
25. Nori, F. and J. P. Rodriguez, "Acoustic and electronic properties of one-dimensional quasicrystals," *Phys. Rev. B*, Vol. 34, 2207, 1986.
26. Fujiwara, T., M. Kohmoto, and T. Tokihiro, "Multifractal wave functions on a Fibonacci lattice," *Phys. Rev. B*, Vol. 40, 7413, 1989.
27. Lusk, D., I. Abdulhalim, and F. Placido, "Omnidirectional reflection from Fibonacci quasi-periodic one-dimensional photonic crystal," *Opt. Commun.*, Vol. 198, 273–279, 2001.

28. Cojocaru, E., "Omnidirectional reflection from finite periodic and Fibonacci quasi-periodic multilayers of alternating isotropic and birefringent thin films," *Appl. Opt.*, Vol. 41, 747, 2002.
29. Aissaoui, M., J. Zaghdoudi, M. Kanzari, and B. Rezig, "Optical properties of the quasi-periodic one-dimensional generalized multilayer Fibonacci structures," *Progress In Electromagnetics Research*, PIER 59, 69–83, 2006.
30. Khalaj-Amirhosseini, M., "Analysis of periodic and aperiodic coupled nonuniform transmission lines using the Fourier series expansion," *Progress In Electromagnetics Research*, PIER 65, 15–26, 2006.
31. Guida, G., "Numerical studies of disordered photonic crystals," *Progress In Electromagnetics Research*, PIER 41, 107–131, 2003.
32. Lakhtakia, A. and C. M. Krowne, "Restricted equivalence of paired epsilon-negative and mu-negative layers to a negative phase-velocity material (alias left-handed material)," *Optik*, Vol. 114, 305, 2003.